ELSEVIER

Journal of Alloys and Compounds 317–318 (2001) 149–152

Journal of ALLOYS AND COMPOUNDS

www.elsevier.com/locate/jallcom

Electronic structure of a hole doped oxide with a quasi-1D crystal structure $Y_{2-x}(Sr,Ca)_xBaNiO_5$

F.-X. Lannuzel[a,*], E. Janod[a], C. Payen[a], G. Ouvrard[a], P. Moreau[a], O. Chauvet[a], P. Parent[b], C. Laffon[b]

[a]*Institut des Matériaux Jean Rouxel, UMR 6502 CNRS-Université de Nantes, 2 rue de la Houssinière, BP 32229, 44322 Nantes Cedex 3, France*
[b]*LURE, Université Paris-Sud, Bâtiment 209D, 91405 Orsay, France*

Abstract

The effect of hole doping into the divalent nickel oxide Y_2BaNiO_5, which provides a good example of one-dimensional electronic structure in the presence of strong d–d interactions, has been examined by means of several techniques including X-ray absorption and electron energy loss spectroscopies at oxygen *K*-edges (O *K*-edges). The crystal structure of this compound shows one-dimensional chains of vertex-sharing NiO_6 octahedra running along the *z*-axis. Hole doping into this material is realized by substituting Ca^{2+} or Sr^{2+} ions for the Y^{3+} ions. We suggest that the doped holes have antibonding Ni $3d(3z^2-r^2)$–O2p(z) character.

Keywords: Nickel oxide; Electronic structure; Hole doping; X-ray absorption

1. Introduction

Electronic structure and physical properties of late 3d transition metal (TM) oxides have attracted considerable attention in recent years, arising from several puzzling issues such as the nature of their ground states and the influence of hole doping. It is now well known that the d–d Coulomb correlation effects play a crucial role in understanding the properties of these oxides. Due to these strong many-body effects, one-electron approaches, such as the density functional theory (DFT), fail to predict the insulating and magnetic properties of, for instance, divalent nickel and copper oxides. A commonly accepted basis for discussion of the electronic structure of TM oxides, which includes correlation effects, is the ionic picture introduced by Zaanen, Sawatzky, and Allen (ZSA) [1]. This model describes the electronic structure in terms of two parameters: the on-site TM Coulomb interaction U and the energy Δ required to transfer an electron from a ligand valence orbital to the TM 3d shell. Within this framework, it is generally accepted that the charge gap in late TM oxides is not of d–d (Mott–Hubbard) type but rather of a O2p–TM3d charge transfer type ($\Delta<U$). This is an important conclusion for understanding the properties associated with hole doping, such as the superconductivity in cuprates. In this simplified picture, one tacitly assumes that possible chemical bonding effects arising from TM3d–O2p interactions play only a minor role.

In this context, the divalent nickel oxide Y_2BaNiO_5 is a good candidate for examining the interplay of correlation and chemical bonding. This compound has an orthorhombic structure (S.G. *Immm*) with isolated one-dimensional chains of vertex-sharing NiO_6 octahedra running along the *z*-axis [2,3]. The NiO_6 octahedra are compressed along the *z* direction. This leads to the presence of two short apical Ni–O bond distances (~1.88 Å) and provides evidence for the existence of significant Ni $3d(3z^2-r^2)$–O2p(z) interactions. Nevertheless, the ground state has insulating properties with a large optical gap of about 2.3 eV [4], arising from the presence of strong d–d electron interactions. Hole doping by the random substitution of Ca^{2+} in place of Y^{3+} has dramatic effects both on the physical properties and the electronic structure [4–6]. X-ray absorption (XAS) and photoemission studies have shown the existence of new empty states in the charge gap region, which have primarily either O2p(z) or mixed Ni $3d(3z^2-r^2)$–O2p(z) character [4,6].

In the present paper, we investigate the changes in the

*Corresponding author. Tel.: +33-2-40-373-952; fax: +33-2-40-373-995.

E-mail address: lannuzel@cnrs-imn.fr (F.-X. Lannuzel).

0925-8388/01/$ – see front matter
PII: S0925-8388(00)01337-2

electronic structure and physical properties on doping holes into Y_2BaNiO_5. In order to isolate universal properties from the aspects that could depend more on the detailed chemistry of the substituted compounds, we have synthetized a new series of samples in which Y^{3+} are replaced by Sr^{2+}. Ca or Sr-containing samples have been characterized by means of several techniques including XAS and electron energy loss spectroscopy (EELS) at oxygen *K*-edges (O *K*-edges).

2. Experimental details

Polycrystalline samples of $Y_{2-x}(Sr,Ca)_xBaNiO_5$ were prepared through standard solid state reactions and characterized by X-ray powder diffraction (XRD), energy-dispersive X-ray analysis (EDX), and thermogravimetric (TG) analysis under reducing conditions. Quantitative elemental analyses were performed on a Cameca electron microprobe at IFREMER (Brest, France).

Electrical resistivities were measured by a standard four probe d.c. method on sintered pellets. Electrical contacts were made with silver paste. Magnetic susceptibilities were measured with a commercial Quantum Design SQUID magnetometer.

Oxygen *K*-edge photoabsorption measurements were performed on the SA22 beamline at LURE (Orsay) using a bulk-sensitive fluorescence-yield-detection method. The monochromator resolution was set at 0.40 eV.

EELS experiments were carried out at 100 kV with an HF2000-FEG transmission electron microscope. The data were collected at 0.1 eV/channel using a GATAN 666 PEELS spectrometer and the analysis mode of the microscope. The zero loss full width at half maximum was 0.75 eV. Read out noise and dark current were subtracted from the spectra.

3. Results and discussion

Pure samples could be obtained for $x_{Ca} \leq 0.2$ and $x_{Sr} \leq 0.2$. Elemental microprobe analyses for Y, Ca, Sr, Ba, and Ni are in excellent agreement with the nominal contents and show very weak dispersion of the Ca or Sr contents for each substituted sample. For each sample, the TG analysis in a H_2/N_2 flow indicates the existence of very weak excess oxygen. The weight loss corresponds to $0.01 \leq \delta \leq 0.02$ for $Y_{2-x}(Sr,Ca)_xBaNiO_{5+\delta}$.

X-ray powder diffraction data were indexed on the basis of an orthorhombic unit cell (S.G. *Immm*). Lattice parameters were evaluated using the least squares refinement method (see Table 1). The results obtained for the Ca series compare well with those in the published literature [5,7]. The most striking feature of the results in Table 1 concerns the *a* parameters, which decrease continuously with increasing x_{Ca} or x_{Sr}. This contraction is surprising if one considers that the ionic sizes of Ca^{2+} and Sr^{2+} are larger than that of Y^{3+} (0.99 Å for Ca^{2+}, 1.13 Å for Sr^{2+}, and 0.93 Å for Y^{3+} [8]). Previous analyses for the Ca compounds [5,7,9], based on the results of powder diffraction and EXAFS studies, have shown that the decrease of the *a* parameter corresponds to the decrease of the Ni–O bond distance along the chain direction (parallel to [100]). This effect is most probably related to the antibonding character of the states in which doped hole reside, as discussed below.

Table 1
Lattice parameters and unit cell volumes for $Y_{2-x}(Sr,Ca)_xBaNiO_5$

x	*a* (Å)	*b* (Å)	*c* (Å)	*V* (Å^3)
$Y_{2-x}Sr_xBaNiO_5$				
0.0	3.7605(9)	5.7601(15)	11.3252(24)	245.3(2)
0.05	3.7588(6)	5.7651(9)	11.3311(18)	245.5(1)
0.10	3.7574(6)	5.7680(9)	11.3373(18)	245.7(1)
0.15	3.7556(9)	5.7713(15)	11.3409(27)	245.8(2)
0.20	3.7542(9)	5.7742(15)	11.3456(24)	245.9(2)
$Y_{2-x}Ca_xBaNiO_5$				
0.05	3.7583(10)	5.7615(14)	11.3245(28)	245.2(2)
0.10	3.7563(12)	5.7648(21)	11.3167(37)	245.1(2)
0.15	3.7530(9)	5.7644(12)	11.3087(27)	244.6(2)

Hole doping into the structure has also important effects on the transport and magnetic properties [6]. For the undoped phase, our data for the temperature dependent resistivity show a thermally activated regime above 140 K, $\rho = \rho_0 \exp(\Delta_g / 2k_B T)$, with $\Delta_g \sim 0.5$ eV. This value is significantly smaller than the observed optical gap (2.3 eV [4]), probably due to weak excess oxygen. For doping levels as low as $x_{Ca,Sr} = 0.05$, we have observed a reduction of the resistivity by two orders of magnitude at 300 K.

The magnetic properties of the pure compound Y_2BaNiO_5 are those of a quasi-1D Heisenberg antiferromagnet with a superexchange parameter $J \approx 280$ K between $S=1$ spins and a quantum (Haldane) spin gap $\Delta_S \approx 100$ K [6]. The susceptibility $\chi(T)$ curve (shown in Fig. 1) has a broad maximum near 400 K. At low temperatures, one observes the exponential decrease of $\chi(T)$ expected for a spin-gap system, which is balanced below 25 K by a Curie-like tail. Hole doping into the magnetic chains leads to complex behavior for the magnetic susceptibility, as is evident from Fig. 1. New magnetic states with effective spins *S* larger than $S=1/2$ per Ca or Sr are created inside the Haldane gap [6]. Spin-glass like behaviors are observed for the Ca-containing samples [10] but not for the Sr series (see Fig. 1). A more detailed analysis of the magnetic properties will appear elsewhere.

We now turn to the effects of hole doping on the charge excitation spectra. The unoccupied part of the electronic structure was investigated by means of XAS and EELS. Fig. 2 shows the O *K*-edge X-ray absorption spectra for the pure phase and two doped compounds. The spectra are normalized to have the same intensity at photon energies of 540 eV. The spectra reveal two distinct pre-edges peaks

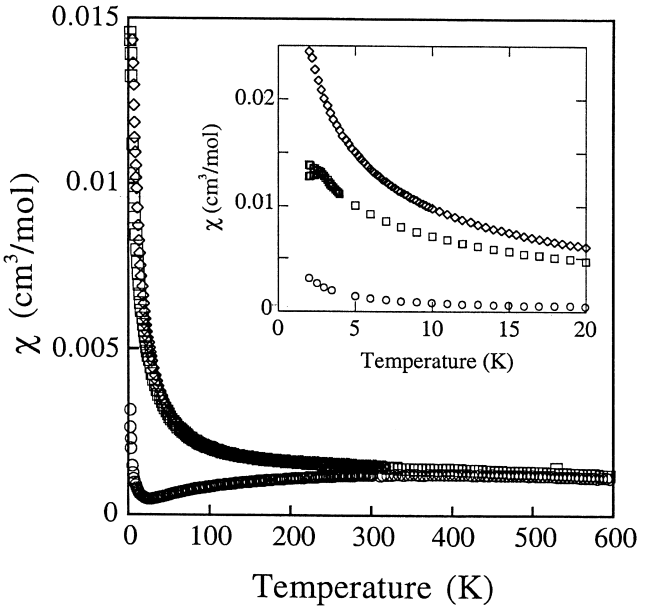

Fig. 1. Magnetic susceptibility vs. temperature, $\chi(T)$, for Y_2BaNiO_5 (circles), $Y_{1.85}Ca_{0.15}BaNiO_5$ (squares), and $Y_{1.8}Sr_{0.15}BaNiO_5$ (diamonds).

(labeled A and B) which evolve systematically as a function of Sr or Ca concentration. The lower peak A, absent for the undoped compound, grows in intensity with the Ca or Sr concentration, while the upper peak B loses intensity. The energy separation between the two peaks is comparable to the optical gap in the insulating $x=0$ phase. These two peaks are also observed in the EELS spectra (see Fig. 3).

All these features have been observed in other hole doped nickel oxides, such as $Li_xNi_{1-x}O$ [11]. Within the ZSA picture, the pre-peak B can be attributed to the transition from the O 1s core level to the d^9 upper Hubbard

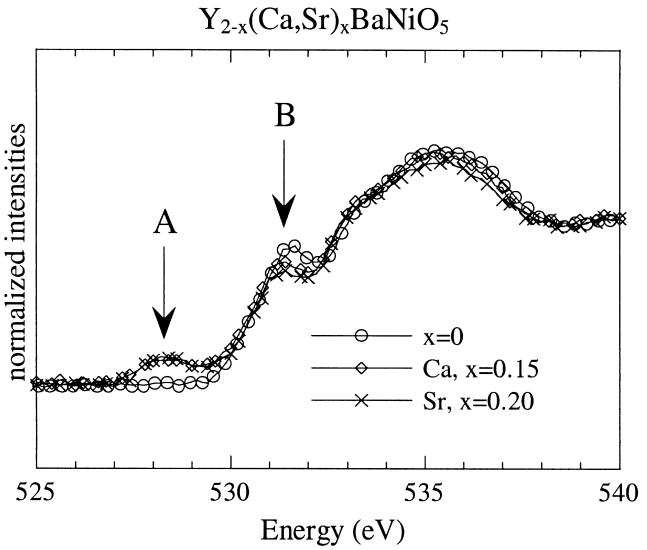

Fig. 2. Oxygen *K*-edge fluorescence yield X-ray absorption spectra for Y_2BaNiO_5, $Y_{1.85}Ca_{0.15}BaNiO_5$ and $Y_{1.8}Sr_{0.2}BaNiO_5$.

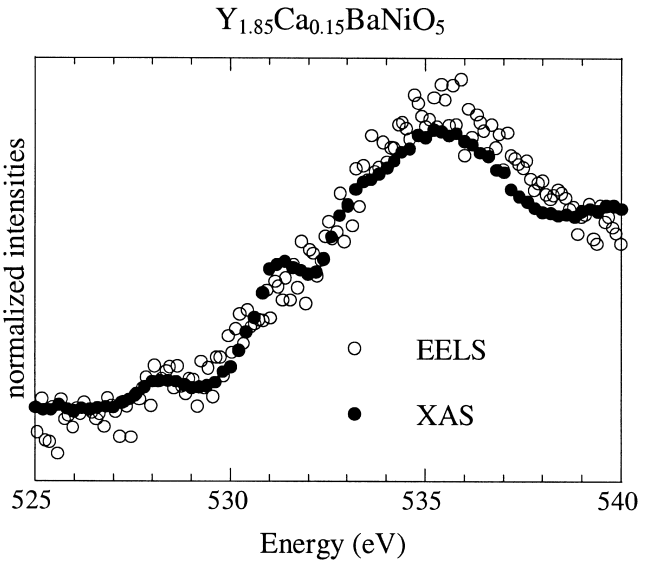

Fig. 3. Oxygen *K*-edge X-ray absorption and electron energy loss spectra for $Y_{1.85}Ca_{0.15}BaNiO_5$.

band. This peak gets its transition probability from the O2p–Ni3d hybridization. The new peak A is attributed to the hole states introduced by the chemical doping, and these states should have significant O2p character. The observed spectral transfer between peaks A and B is expected for a charge-transfer system with significant TM3d–O2p hybridization (it is also expected for a Mott–Hubbard system even in the absence of hybridization) [12]. For $Li_xNi_{1-x}O$, it has been suggested that these holes are of primarily O2p character, in agreement with the charge-transfer nature suggested for the band gap of NiO [11].

The situation is probably different for Y_2BaNiO_5, because of the low-dimensionality of its crystal structure and the presence of strong Ni $3d(3z^2-r^2)$–O2p(z) interactions. Indeed, the nickel-apical oxygen distance in Y_2BaNiO_5 is very short (~1.88 Å) compared with the distance observed in NiO (~2.08 Å). According to a recent photoemission study, the doped holes in Y_2BaNiO_5 have mixed Ni $3d(3z^2-r^2)$–O2p(z) character [4]. Also, the results of XAS measurements at Ni *K*-edge for the Ca compounds seem to indicate an increase in the concentration of the formal Ni^{3+} oxidation state when the doping level increases [9]. Nevertheless, the contraction of the Ni–O distance along the chain direction (parallel to [100]) is attributable to the antibonding character of the doped hole states, rather than to the presence of nickel ions in a pure ionic Ni^{3+} state. This assumption is based on the results of a nonmagnetic LAPW band structure calculation of the pure compound, for which the Fermi level cuts an antibonding σ^* combination of Ni $3d(3z^2-r^2)$ and O2p(z) orbitals [13]. Although this calculation fails to predict the experimentally observed insulating ground state, because of the strong d–d correlations, it should be accurate with respect to the gross features of the charge distribution.

4. Conclusion

In this work, we have synthesized and characterized a new hole doped quasi-1D system, $Y_{2-x}Sr_xBaNiO_5$. Based on literature and our results from X-ray diffraction, XAS and EELS, we propose that holes enter primarily an antibonding σ^*_Z ($O2p_z$–$Ni3d_{z2}$) band. Spectral weight transfers from the upper Hubbard band to excitations with lower energies are observed in the O 1s XAS spectra. This latter observation is, in fact, a general feature of doped charge-transfer insulators, suggesting that the main characteristics of the unoccupied part of the charge spectrum of these systems are not very sensitive to the dimensionality of the crystal structure. On the other hand, the transport and magnetic properties of $Y_{2-x}(Sr,Ca)_xBaNiO_5$ are strongly affected by the quasi-1D nature of the TM–O–TM network.

Acknowledgements

We wish to thank A. Barreau (Nantes) and M. Bohn (IFREMER, Brest) for the EDX and electron microprobe analyses.

References

[1] J. Zaanen, G.A. Sawatsky, J.W. Allen, Phys. Rev. Lett. 55 (1985) 418.
[2] J. Amador, E. Gutiérrez-Puebla, M.A. Monge, I. Rasines, C. Ruíz-Valero, F. Fernández, R. Sáez-Puche, J.A. Campá, Phys. Rev. B 42 (1990) 7918.
[3] D.J. Buttrey, J.D. Sullivan, A.L. Rheingold, J. Solid State Chem. 88 (1990) 291.
[4] K. Maiti, D.D. Sarma, Phys. Rev. B 58 (1998) 9746.
[5] J.A. Alonso, I. Rasines, J. Rodriguez-Carvajal, J.B. Torrance, J. Solid State Chem. 109 (1994) 231.
[6] J.F. Di Tusa, S.W. Cheong, J.-H. Park, G. Aeppli, C. Broholm, C.T. Chen, Phys. Rev. Lett. 73 (1994) 1857.
[7] V. Massarotti, D. Capsoni, M. Bini, A. Altomare, A.G.G. Moliterni, Z. Kristallogr. 214 (1999) 205.
[8] R.D. Shannon, Acta Cryst. A32 (1976) 751.
[9] R. Castaner, C. Prieto, A. De Andres, J.L. Martinez, R. Sáez-Puche, J. Alloys Comp. 210 (1995) 31.
[10] K. Kojima, A. Keren, L.P. Le, G.M. Luke, B. Nachumi, W.D. Wu, Y.J. Uemura, K. Kiyono, S. Miyasaka, H. Takagi, S. Uchida, Phys. Rev. Lett. 74 (1995) 3471.
[11] P. Kuiper, G. Kruizinga, J. Ghijsen, G.A. Sawatsky, H. Verweij, Phys. Rev. Lett. 62 (1989) 221.
[12] H. Eskes, M.B.J. Meinders, G.A. Sawatsky, Phys. Rev. Lett. 67 (1991) 1035.
[13] L.F. Mattheiss, Phys. Rev. B 48 (1993) 4352.